Tetrahedron 67 (2011) 2794–2802

Contents lists available at ScienceDirect

Tetrahedron

journal homepage: www.elsevier.com/locate/tet

Chromogenic and fluorogenic sensing of Cu^{2+} based on coumarin

Aasif Helal [a], Mohammad Harun Or Rashid [b], Cheol-Ho Choi [b], Hong-Seok Kim [a,*]

[a] Department of Applied Chemistry, Kyungpook National University, Daegu 702-701, Republic of Korea
[b] Department of Chemistry, Kyungpook National University, Daegu 702-701, Republic of Korea

ARTICLE INFO

Article history:
Received 9 December 2010
Received in revised form 31 January 2011
Accepted 31 January 2011
Available online 4 March 2011

Keywords:
Fluorescence sensor
Chromogenic sensing
Copper ion
Thiazole
Coumarin

ABSTRACT

A new highly selective, reversible, chromogenic, and fluorogenic chemosensor (**4**) based on thiazole–coumarin moieties for quantification of copper ions in aqueous-DMSO was designed and synthesized. The mechanism of fluorescence was based on ICT, which was modified by the introduction of an electron-donating diethylamino group making it chromogenic and increasing the binding affinity. The selectivity toward copper ions was not affected by the presence of representative alkali metals, alkali earth metals, or other transition metals.

1. Introduction

The design and synthesis of chemosensors for highly noxious, heavy, and transition metal ions are currently a task of prime importance for medical, environmental, and biological applications.[1] Presently, one of the most attractive approaches focuses on the research of novel colorimetric and fluorescent metal ion sensors, which allow naked-eye detection of color and fluorescent emission change upon metal ion binding without the use of a spectroscopic instrument.[2] Copper plays an important role in various biological processes. It is a vital trace element, the third most abundant in humans, and is present at low level in a variety of cells and tissues, with the highest concentration in the liver. The average concentration of blood copper in the normal group is 100–150 μg/dL (15.7–23.6 μM).[3] Its concentration in the neuronal cytoplasm may contribute to the etiology of Alzheimer's or Parkinson's disease.[4,5] The U.S. Environmental Protection Agency (EPA) has set the limit of copper in drinking water to be 1.3 ppm (~20 μM). As a pollutant due to its extensive industrial use and an essential trace element in biological systems, chemosensors for copper(II) based on chromogenic probes that are expected to quickly, nondestructively, and sensitively detect copper ions have drawn a lot of attention.[2a,6] So far, only a few colorimetric and fluorescent sensors based on the rhodamine chromophore for copper ions have been reported. However, only few of them exhibit good performance in aqueous media, which is a very important factor for potential biological applications.[7]

In chemosensors, a selective binding motif is attached to a fluorophore for signal transduction. However, one disadvantage is that the recognition event is sometimes difficult to detect because the fluorophore does not directly contact the bound metal ion. In this aspect, an ideal fluorescent probe would be one whose fluorescent unit is directly involved in the interaction with the metal ions. We choose coumarin as the fluorophore due to its desirable photophysical properties, such as a large Stokes shift, visible excitation and emission wavelengths, and a structure that can be easily modified.[8] Moreover, the carbonyl group of coumarin can take part in the coordination with metal ions.

It is known that chelating groups such as C=N and C=O exhibit a high affinity to transition and post-transition metal cations, but less binding affinity toward alkali metal and alkaline earth metal cations.[9] The carbon in the 3-position bears a partial negative charge in the ground state for all of the coumarins. Intramolecular charge transfer (ICT) would be facilitated by attachment of an electron-withdrawing substituent at the 3-position.[10] Introduction of a thiazole ring at the 3-position of a coumarin moiety enhances the ICT because of the stronger electron-withdrawing ability of the thiazole ring. Thus a heteroaromatic ring system, such as a thiazole with a coumarin as a fluorophore at position 4 and a phenol at position 2 can chelate with metal ions via the carbonyl oxygen, thiazole nitrogen, and phenol oxygen atoms that act as a –ONO– donor receptor moiety highly selective for copper.[11]

Recently, thiazole based chemosensors **1** and **2**, as shown in Fig. 1, with a phenol at the 2 position and pyridine (**1**) or another

* Corresponding author. Tel.: +82 53 950 5588; fax: +82 53 950 6594; e-mail address: kimhs@knu.ac.kr (H.-S. Kim).

0040-4020/$ – see front matter © 2011 Elsevier Ltd. All rights reserved.
doi:10.1016/j.tet.2011.01.093

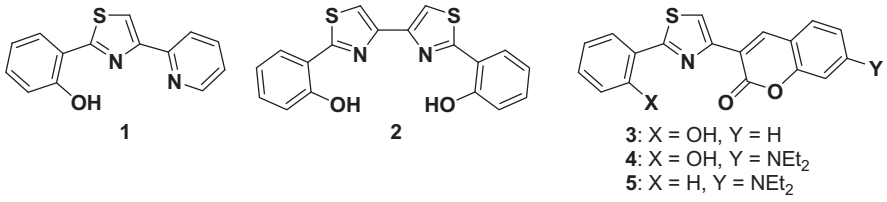

Fig. 1. Structures of chemosensors.

thiazole phenol moiety (**2**) at the 4 position of the thiazole ring, for ratiometric fluorescence sensing of zinc[12] and dual sensing of copper and zinc have been reported.[13] In both of these cases, soft heteroatoms, such as N and S, as an electron donor to metal cations along with phenolic oxygen, improved the binding selectivity with zinc and copper.

This paper describes a new coumarin fluorophore at the 4 position of the thiazole ring. Its reversible, highly selective, chromogenic, fluorogenic responses upon the addition of copper ions and competititive behavior with other cations in aqueous-DMSO (3:1) containing HEPES buffer (10 mM, pH 7.4) are demonstrated.

2. Results and discussion

Due to the high affinity of Cu^{2+} ions for electron-donating nitrogen and carbonyl oxygen during complexation, two thiazole-coumarin based analogs—2-(2′-hydroxyphenyl)-4-(3′-coumarinyl)thiazole (**3**) and 2-(2′-hydroxyphenyl)-4-[(3′-(7-diethylaminocoumarinyl)]thiazole (**4**)—were synthesized in order to compare the metal ion selectivity and sensitivity. To understand the crucial role of both the phenol and coumarin providing a suitable binding site for Cu^{2+}, 2-phenyl-4-[(3′-(7-diethylaminocoumarinyl)]-thiazole (**5**) was also prepared. Sensors **3** and **4** were obtained by reacting 2-hydroxythiobenzamide (**6**) with 3-(2-bromoacetyl)coumarin (**7**) and 3-(2′-bromoacetyl)-7-diethylaminocoumarin (**8**), respectively, and **5** was obtained by reaction of thiobenzamide (**9**) with **8** in refluxing ethanol as shown in Scheme 1. The 2-hydroxy-thiobenzamide (**6**) was prepared by thionation of 2-hydroxy-benzamide with Lawesson's reagent. The 3-(2′-bromoacetyl)-7-diethylaminocoumarin (**8**) was prepared by a condensation reaction of 4-(diethylamino)salicylaldehyde with ethyl acetoacetate in ethanol followed by bromination.[14] The structures of **3**, **4**, and **5** were confirmed by ^1H NMR, ^{13}C NMR, and elemental analysis.

Initial studies on the UV–vis absorption and fluorescent emission revealed that **3** showed selectivity toward Cu^{2+} ions in aqueous-DMSO (3:1 v/v). In the absence of Cu^{2+} ion, **3** showed an absorption band at 346 nm, that is, attributed to the $n\rightarrow\pi^*$ transitions of the coumarin moiety. On addition of Cu^{2+} to the solution of **3** chelation with the carbonyl of the coumarin enhances the electron-withdrawing character of the acceptor carbonyl moiety, resulting in the formation of a new red-shifted absorption band at 375 nm (Table 1) and synchronous decrease in the absorption band at 346 nm, as shown in Fig. 2b. The absorption bands at 346 and 375 nm linearly decreased and increased, respectively, up to 1 equiv of Cu^{2+} ion addition (Fig. 2b inset), indicating the formation of a 1:1 complex. None of the other cations produced such a redshift in their absorption spectra (Fig. 2a).

Table 1
Comparisons of the absorption, emission, and binding properties of sensors **3** and **4** in H_2O–DMSO (3:1)

	3	**3**+Cu^{2+}	Δλ (nm)	**4**	**4**+Cu^{2+}	Δλ (nm)
λ_{max} (nm)	346	375	29	412	460	48
log ϵ	3.6	3.9		4.3	4.2	
λem (nm)	460	460		495	0	
I/I_0		0.3			0.0	
Φ^a	0.01			0.35		
K_a		4.4×10^4			2.2×10^6	

[a] Quantum yields were obtained using quinine sulfate in 0.5 M H_2SO_4 as standard.

Fluorescence spectra of **3** in aqueous-DMSO (3:1 v/v) showed the emission peak at 460 nm corresponding to the charge transfer (CT) from the phenol and thiazole to the coumarin moiety (Fig. S9). On the addition of Cu^{2+} up to 1 equiv the emission peak is partially quenched, but no further quenching occurred upon the addition of the analyte up to 10 equiv (Fig. 3b). From fluorescence titration the binding constant of **3** with Cu^{2+} was calculated to be $4.4\times10^4\ M^{-1}$

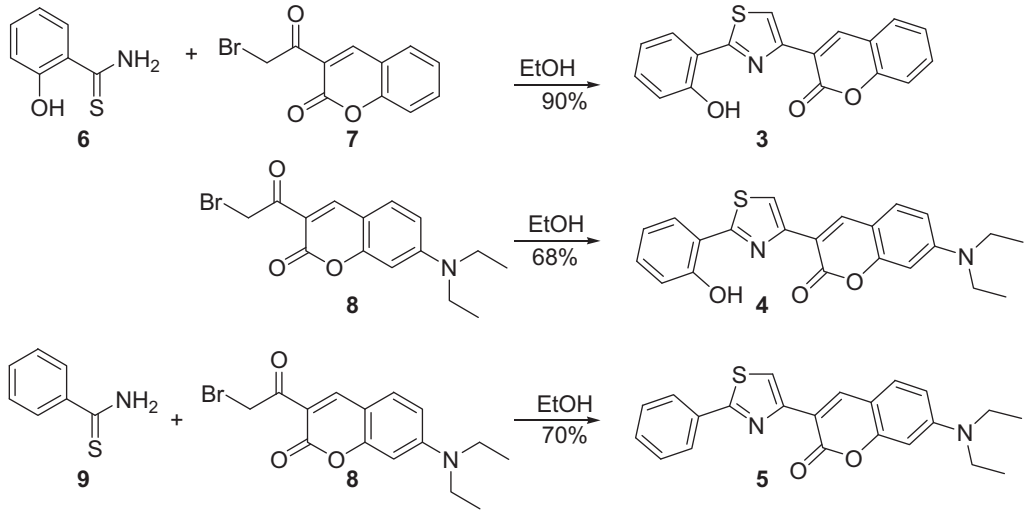

Scheme 1. Synthesis of **3**, **4**, and **5**.

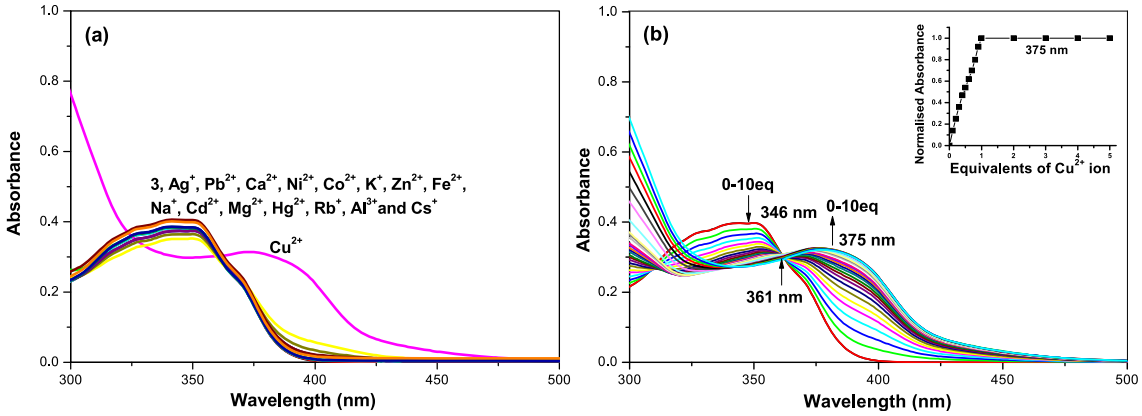

Fig. 2. UV–vis spectra of **3** (20 μM) (a) with different cations (10 equiv), (b) upon the addition of $Cu(ClO_4)_2$ (200 μM) in H_2O–DMSO (3:1) containing HEPES buffer (10 mM, pH 7.4). Inset: mol ratio plot of absorbance at 375 nm.

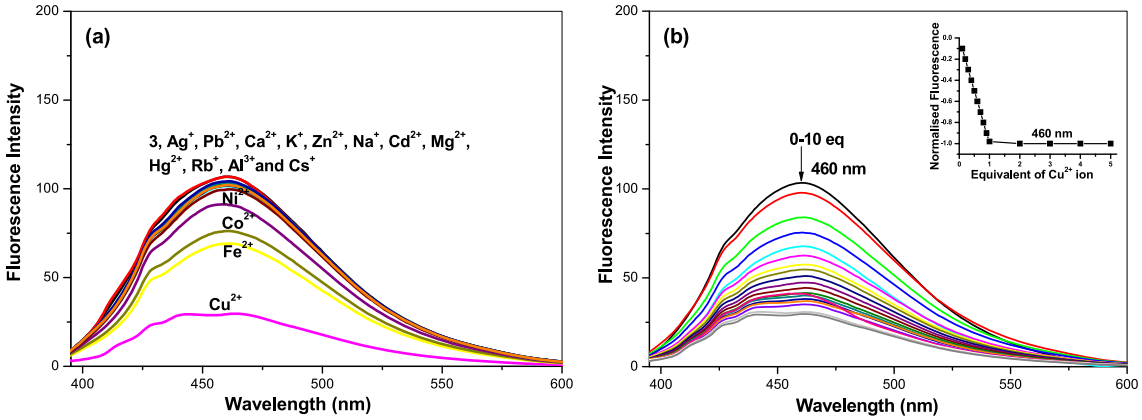

Fig. 3. Fluorescence spectra of **3** (20 μM) in H_2O–DMSO (3:1) containing HEPES buffer (10 mM, pH 7.4) (a) upon the addition of 10 equiv of various metal cations, (b) as a function of added $Cu(ClO_4)_2$. Inset: mol ratio plot of emissions at 460 nm (λ_{ex}=361 nm).

(error limits ≤10%) (Fig. 7a).[15] Moreover, iron and cobalt ions also partially quench the fluorescence of **3** (Fig. 3a).

To enhance the fluorescence intensity, quantum yield, binding ability and selectivity toward Cu^{2+}, an electron-donating diethylamino group was introduced into coumarin at the 7-position in conjugation with the electron-withdrawing carbonyl group. This increases the CT character by producing a large change in the dipole moment upon excitation from the ground to the excited state resulting in very large Stokes' shifts between their absorption and fluorescence maxima,[16] increasing the molar extinction coefficient of the sensor in the free and complex forms, and in the binding constant (Table 1).[17]

UV–vis properties of **4** were investigated in aqueous-DMSO (3:1) at a concentration level of 20 μM. Compound **4** displayed an obvious absorption band in the visible region peaked at 412 nm, which could be assigned to the CT absorbance, as observed in other compounds with ICT character (Fig. 4). However, upon the addition of Cu^{2+} to the solution of **4** a new red-shifted absorption band at 460 nm is enhanced gradually while the absorption band at 412 nm decreased synchronously, with an isobestic point at 435 nm as

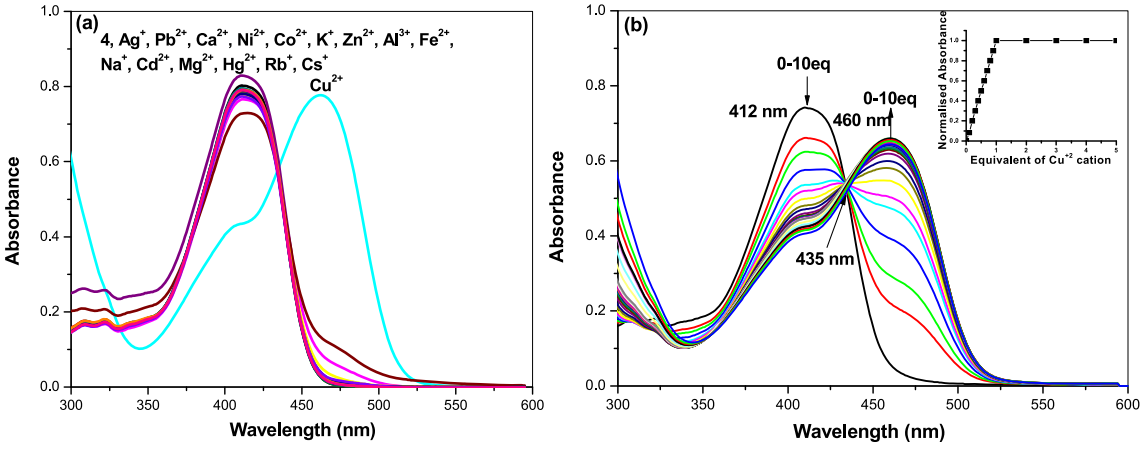

Fig. 4. UV–vis spectra of **4** (20 μM) (a) with different cations (10 equiv), (b) upon the addition of $Cu(ClO_4)_2$ (200 μM) in H_2O–DMSO (3:1) containing HEPES buffer (10 mM, pH 7.4). Inset: mol ratio plot of absorbance at 460 nm.

shown in Fig. 4b. The absorption bands at 412 and 460 nm linearly decreased and increased, respectively, up to 1 equiv of Cu^{2+} (Fig. 4b inset), indicating the formation of a 1:1 complex with a strong binding affinity. The Job's plot of **4** with Cu^{2+} also confirmed the formation of a 1:1 complex (Fig. S1). The changes in the absorption spectra upon the complexation are due to the direct interaction between the bound cation and the carbonyl group of the coumarin moiety. The Cu^{2+} ion reinforces the electron-withdrawing character of the carbonyl group in coumarin, which leads to a bathochromic shift of 48 nm in the absorption spectrum (Table 1). In terms of electronic interaction, the dipole moment of 7-diethylaminocoumarin in the excited state is higher than that of the ground state because of the photoinduced CT occurring from the diethylamino, a nonbonding electron donor group, to the carbonyl group. Therefore, when Cu^{2+} ions coordinate with the carbonyl group, the excited state is more stable than the ground state so that the absorption spectrum is shifted toward the red. In this intrinsic chromogenic sensor, the ligand–Cu^{2+} binding was accompanied by the solution color change from light green to yellow, which is easily observed by the naked-eye (Fig. 5a). This response was selective for Cu^{2+} under these conditions. The addition of 10 equiv of the other cations as their perchlorate salts resulted in no appreciable changes (Fig. 4a).

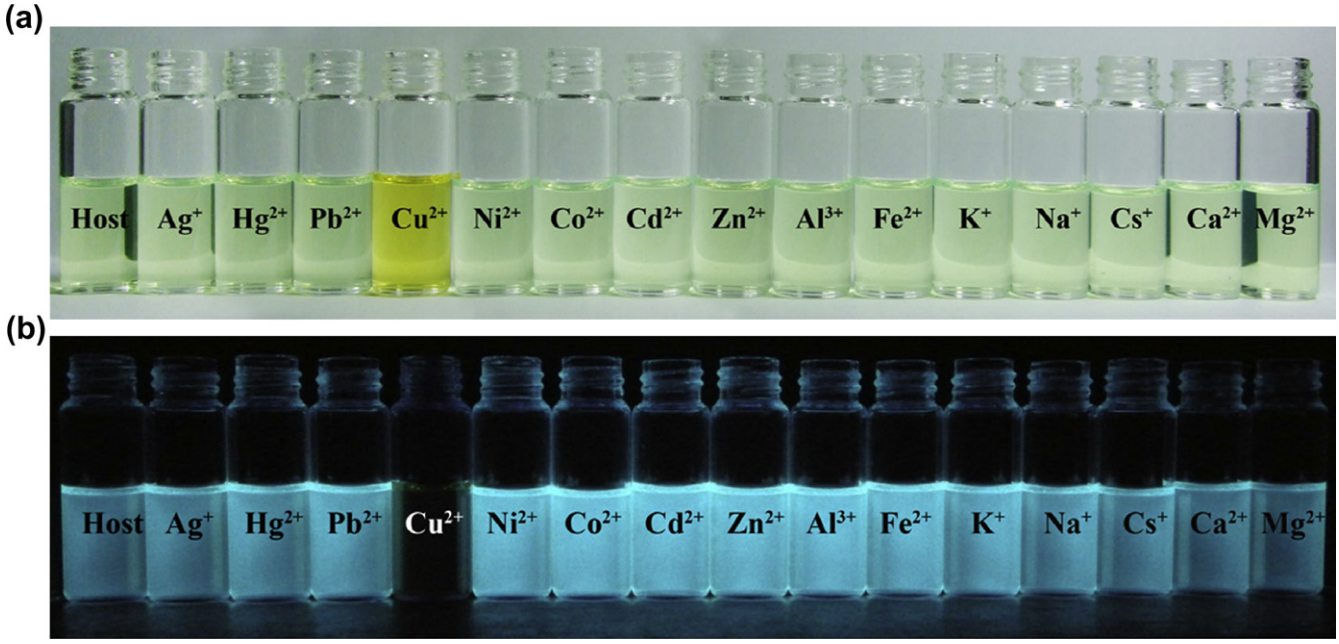

Fig. 5. (a) Chromogenic changes of a 20 μM solution of **4** in H_2O–DMSO (3:1) containing HEPES buffer (10 mM, pH 7.4) in the presence of 10 equiv of each cation. (b) Fluorogenic changes of a 20 μM solution of **4** in H_2O–DMSO (3:1) containing HEPES buffer (10 mM, pH 7.4) in the presence of 10 equiv of each cation upon illumination at 365 nm.

Similarly, fluorescence titration of **4** with Cu^{2+} was carried out in aqueous-DMSO (3:1) at a concentration level of 0.2 μM. The addition of Cu^{2+} to the solution of **4** causes a complete quenching of the fluorescent emission and the peak at 495 nm is *switched off* when excited at 435 nm (Figs. 5b and 6b). The long wavelength of excitation (435 nm) and emission (495 nm) can prevent damage to living biological samples, interference by autofluorescence from native cellular species, and the influence of background fluorescence.[18] Thus introduction of 7-diethylaminocoumarin, a typical dye with enhanced ICT character, as a fluorophore, increases the absorbance and emission efficiency and the quantum yield of sensor **4** (Φ=0.35) as compared to **3** (Φ=0.01) (Table 1). Cu^{2+}, being a paramagnetic cation with open shell d-orbitals, quenches the fluorescence of the fluorophore upon binding with it. Presumably this is due to the electron or charge transfer between the metal cation and thiazole,

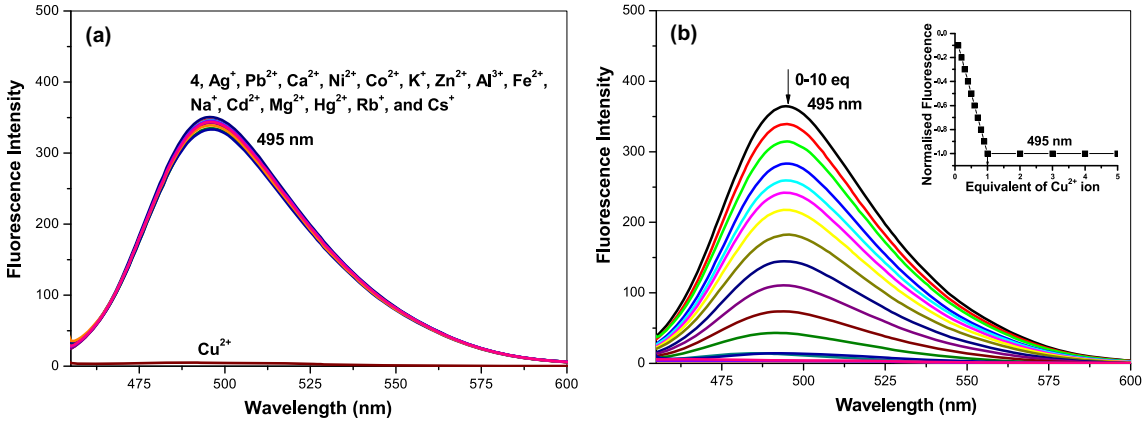

Fig. 6. Fluorescence spectra of **4** (0.2 μM) (a) with different cations (10 equiv) (b) as a function of added $Cu(ClO_4)_2$ in H_2O–DMSO (3:1) containing HEPES buffer (10 mM, pH 7.4). (λ_{ex}=435 nm). Inset: mol ratio plot of emission at 495 nm.

phenol, and coumarin fluorophore providing a very fast and efficient nonradiative decay of the excited state.[2a,19] Compound **4** undergoes a complete quenching of fluorescence (99% quenching) as compared to **3**. The binding mode of **4** with Cu^{2+} from the results of fluorescence titration spectra (Fig. 6b inset) was 1:1 with a binding constant of 2.2 $\times 10^6$ M^{-1} (error limits $\leq$10%) (Fig. 7b).[15]

moiety inhibit the $n \rightarrow \pi^*$ transitions in **3** and the CT in **4**. Further increase of the pH from 5.0 to 6.0 the absorbance reaches its maximum and displays no obvious change in its characteristic within the range of 6.0–9.0. Increasing the pH (10.0–12.0) results in blue shift of the absorbance in both the probes due to the deprotonation of the phenol (Figs. 8a, Figs. S-2a and S-3a).[19c]

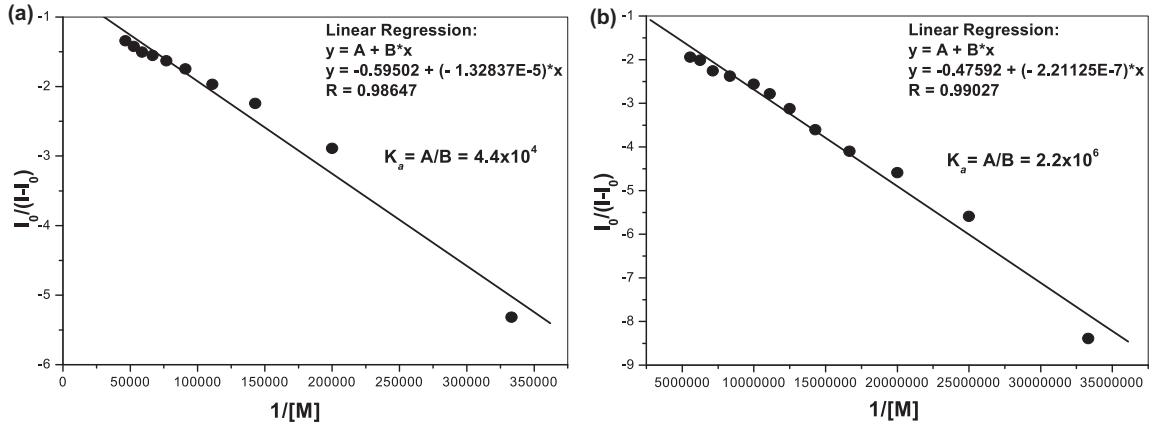

Fig. 7. Linear regression curve of (a) **3** and (b) **4** obtained by plotting $I_0/(I-I_0)$ as a function of $1/[Cu^{2+}]$ in H_2O–DMSO (3:1) containing HEPES buffer (10 mM, pH 7.4). (λ_{ex}=361 nm for **3** and 435 nm for **4**).

The selectivity and tolerance of **4** for Cu^{2+} over other metal cations were investigated by adding 10 equiv of metal cations to 0.2 μM solution of **4**. In the case of Cu^{2+} the molecular fluorescence is quenched to a maximum level and therefore a high molecular sensitivity is attained. Nevertheless, there was no quenching with any other metal ions, as shown in Fig. 6a. This selectivity is due to the fact that although transition metals do not differ too much in size, but they can establish coordinative interactions at very different energies, which can be used for discriminative purposes, especially for fluorescent sensing.[20] This phenomenon is consistent with copper that occurs highest on the Irving–Williams series.[21] Copper(II) has a particularly high thermodynamic affinity for the typical –ONO– donor, i.e., the imino nitrogen of the thiazole ring, carbonyl group of the coumarin moiety, and a strong tendency to promote deprotonation of phenolic proton during complex formation,[9] with fast metal-to-ligand binding kinetics that are not possible with the other transition metal ions.

For the biological application of chemosensors, the sensing should operate in a wide range of pH. So the effects of pH on the absorbance and emission intensities of **3** and **4** in the absence and presence of Cu^{2+} were investigated in the pH range from 2.0 to 12.0 (Fig. 8). Decreasing the pH decreases the absorbance, of **3** at 346 nm and **4** at 412 nm, as the protonation of the thiazole and coumarin

The difference in the absorbance of the probes and its copper complexes is negligible at low (2.0–5.0) and high (10.0–12.0) pH. But at pH 6.0 there is a redshift to 375 nm in **3** and 460 nm in **4** on addition of Cu^{2+} this redshift and the characteristic absorbance were unchanged within the pH range from 6.0 to 9.0 suggesting that the Cu^{2+} complex of both the sensors are stable over this range (Figs. S2b and S3b).

Next the effect of pH on the emission spectrum was investigated (Fig. 8b). In both **3** and **4** decreasing pH protonates the nitrogen of the thiazole ring and the tertiary nitrogen of **4** thus inhibiting the ICT to the coumarin resulting in decrease of fluorescence. At pH 6.0 both **3** and **4** show a maximum intensity and it remain unchanged till pH 9.0. At higher pH (>9.0) the fluorescence intensity is decreased due to the enhancement of negative charge density and formation of phenolate (Figs. S4a, S5a).[19f]

The effect of pH on the Cu^{2+} complex of **3** and **4** shows that increase in pH increases the amount of quenching, reaching its maximum at pH 6.0 after which it displayed no pH-sensitivity till pH 9.0. With further increase of pH, the fluorescence intensity of **3**, **4** and their Cu^{2+} complexes become closer, probably because the formation of hydroxo-complex of Cu^{2+} is favored in this condition (Figs. S4b, S5b).[19f] Thus chemosensors **3** and **4** displayed virtually

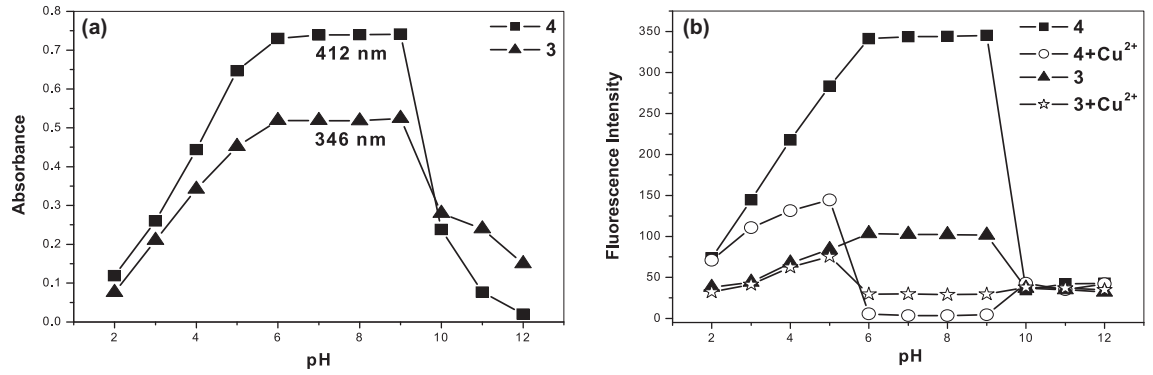

Fig. 8. Effect of pH on the (a) absorbance and (b) emission intensities of **3**, **4** and their Cu^{2+} complexes in H_2O–DMSO (3:1) containing HEPES buffer (10 mM). (λ_{ex}=361 nm for **3** and 435 nm for **4**).

no physiological pH-sensitivity and fluorescence *on–off* can be controlled by Cu^{2+} ion binding within the pH range of 6.0–9.0.

In contrast to **4**, compound **5**, which has no hydroxyl group in the phenyl ring, did not reveal any significant changes in absorption and fluorescence emission upon addition up to 10 equiv of Cu^{2+} ions, as shown in Fig. 9, which indicates the importance of a phenolic group as a binding site at the 2 position of the thiazole ring.

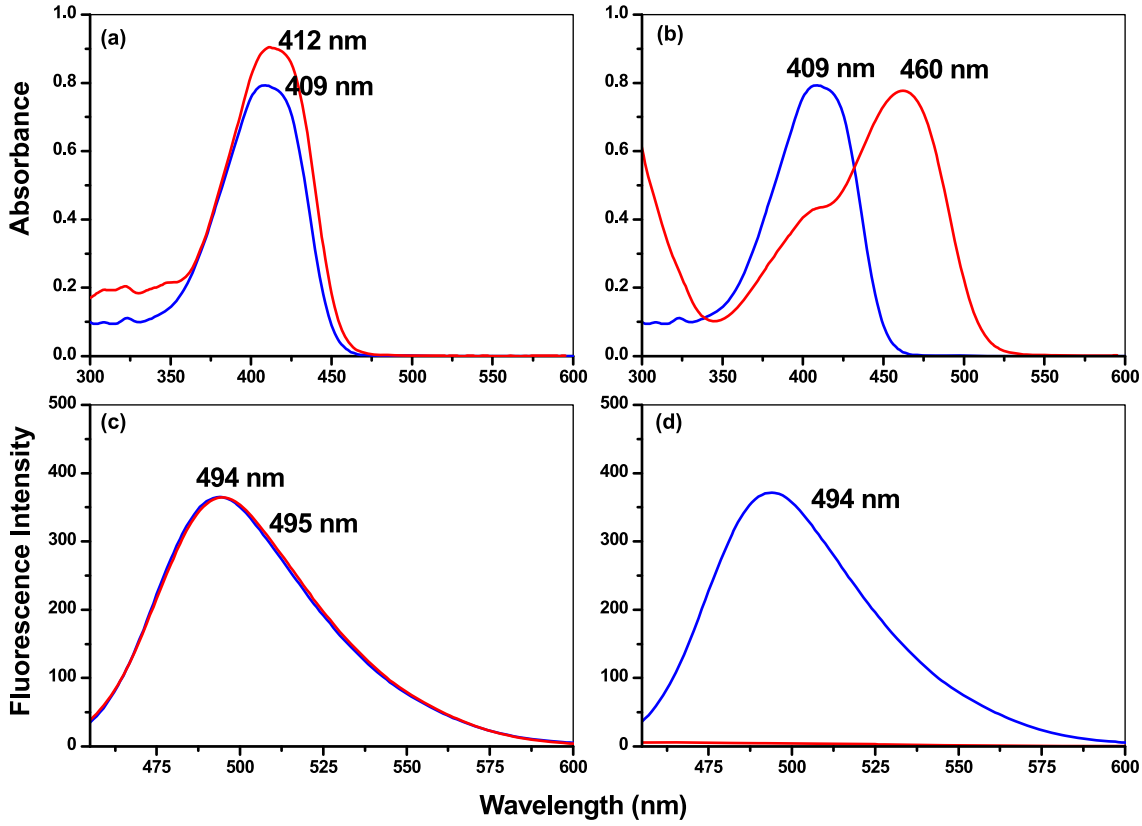

Fig. 9. UV–vis spectra of **4** (—) and **5** (—) (a) in the absence, (b) in presence of 10 equiv of $Cu(ClO_4)_2$ in H_2O–DMSO (3:1) containing HEPES buffer (10 mM, pH 7.4). Fluorescence spectra of **4** (—) and **5** (—) (c) in the absence and (d) in the presence of 10 equiv of $Cu(ClO_4)_2$ in H_2O–DMSO (3:1) containing HEPES buffer (10 mM, pH 7.4).

Competitive binding experiments with different metal ions (10.0 equiv) and Cu^{2+} ion (1.0 equiv) as shown in Fig. 10 showed that they did not interfere with the quenching of Cu^{2+} by **4**. It was also found that **4** shows 0.04 μM of detection limit able to sufficiently sense the Cu^{2+} concentration in the blood system and in drinking water (Fig. S6).[22]

An NMR study for complexation was not available due to the paramagnetic property of Cu^{2+}. Instead, the complex of **4** was prepared with Cu^{2+} in ethanol–DMSO (9:1) and characterized by HR-FAB mass (Fig. S7). The mass spectra of **4**–Cu^{2+} shows a 1:1 stoichiometry (between **4** and Cu^{2+}) with the molecular ion peak at *m*/*z* 532.0557, which corresponds to (**4**+Cu^{2+}+DMSO–H)$^+$. EPR spectroscopic study of the **4**–Cu^{2+} complex showed that the copper retains its oxidation state of 2^+ during complexation (Fig. S8).

To examine the reversibility of **4** toward Cu^{2+}, an aqueous-DMSO (3:1) solution of EDTA (2.0 μM) was added to the complexed solution of **4** (0.2 μM) and Cu^{2+} (2.0 μM). As expected, an absorption peak at 412 nm and a fluorescence signal with a maximum at 495 nm were completely recovered, demonstrating the binding is chemically reversible and not a cation-catalyzed reaction (Scheme 2).

To understand the fluorescence quenching behavior of **3** and **4** upon addition of Cu^{2+} the frontier molecular orbitals [HOMO, LUMO, and SOMO (singly occupied molecular orbital)] of **3**, **4**, **3**–Cu^{2+}, and **4**–Cu^{2+} were calculated. For compound **4**, the HOMO shows that the electrons are distributed over the phenol, thiazole, and coumarin ring. On the other hand the LUMO of **4** shows the density of electrons over the coumarin and thiazole ring, which indicates charge or electron transfer from the phenolic group to a large extent accompanied by charge transfer from the diethylamino group of the coumarin resulting in a peak at 495 nm. On complexation with copper, the SOMO of **4**–Cu^{2+} shows the electron density transferred over the Cu^{2+} ion (Fig. 11). Thus, localization of SOMO over the Cu^{2+} ion causes the fluorescence quenching of **4** upon addition of Cu^{2+}.[6b] The contributions of each electronic oscillator to the lowest energy transition (from the ground state to the first excited state) are listed in Table 2. The electronic oscillators of **4**–Cu^{2+} corresponding to the HOMO→SOMO transitions were calculated to be 54%, which is significantly higher and at such a density change may cause the complex to quench the fluorescence. Thus, the fluorescence quenching behavior is mainly due to the HOMO→SOMO of **4**–Cu^{2+}, which evidently show the photoinduced electron transfer from the thiazole, phenolic, and coumarin ring to the Cu^{2+} ion.

Similar charge transfer from the phenol and thiazole to the coumarin moiety causes fluorescence in **3** and HOMO→SOMO transition in **3**–Cu^{2+} also caused the partial fluorescence quenching (Fig. S9). For this purpose, the TD-B3LYP/6-31G(d) calculated oscillator strength f_1 to the lowest energy transition, are listed in Table 3 that shows that the oscillator strength is at maximum in the case of **4** (f=0.345), which becomes almost zero (f=0.0001) in the lowest energy transition of **4** upon complexation with Cu^{+2} that implies the complete quenching in **4**–Cu^{+2} (Table 3). While in the case of **3**, the fluorescence intensity being less than **4**, the oscillator strength f_1 is sevenfold less (f=0.050) as compared to **4** and in the **3**–Cu^{2+} complex the oscillator strength is fourfold excess (f=0.0004) than **4** resulting in partial quenching.

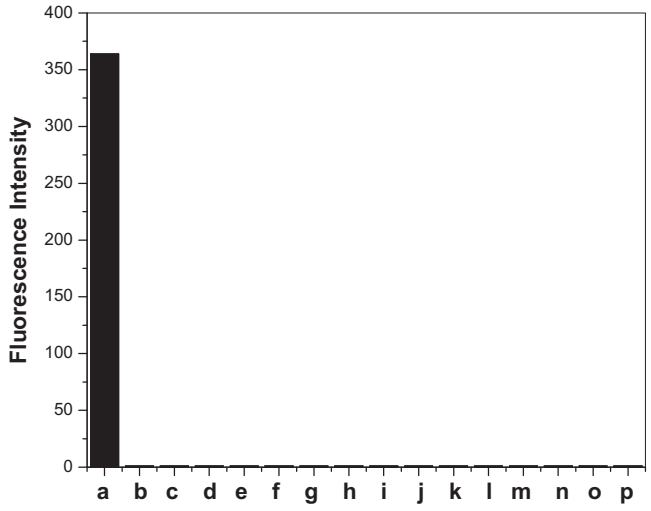

Fig. 10. Metal ion selectivity of (**4**): bars indicate the fluorescence intensity (435 nm excitation, 495 nm emission). Perchlorate salts of various metal ions (10.0 equiv) were added to **4** (0.2 μM) and Cu^{2+} (1.0 equiv) (a) **4** only, (b) $Ag^{+}+Cu^{2+}$, (c) $Pb^{2+}+Cu^{2+}$, (d) $Ca^{2+}+Cu^{2+}$, (e) $Ni^{2+}+Cu^{2+}$, (f) $Co^{2+}+Cu^{2+}$, (g) $K^{+}+Cu^{2+}$, (h) $Zn^{2+}+Cu^{2+}$, (i) $Al^{3+}+Cu^{2+}$, (j) $Fe^{2+}+Cu^{2+}$, (k) $Na^{+}+Cu^{2+}$, (l) $Cd^{2+}+Cu^{2+}$, (m) $Mg^{2+}+Cu^{2+}$, (n) $Hg^{2+}+Cu^{2+}$, (o) $Cs^{+}+Cu^{2+}$, (p) $Rb^{+}+Cu^{2+}$ in H_2O–DMSO (3:1) containing HEPES buffer (10 mM, pH 7.4).

DMSO of analytical grade was purchased from Merck. Deionized water (double distilled) was used throughout the experiment as an aqueous layer. All other materials for synthesis were purchased from Aldrich Chemical Co. and used without further purification. Compounds **7** and **9** were obtained from Aldrich Chemicals, 2-hydroxythiobenzamide (**6**),[12] and 3-(2-bromoacetyl)-7-diethylaminocoumarin (**8**)[14] were prepared by the procedure in the literature. The solutions of metal ions were prepared from their perchlorate salts of analytical grade, and then subsequently diluted to prepare working solutions. HEPES buffer solutions of different pH were prepared using proper amount of HEPES, KOH (1 N), and HCl (1 N) (all of analytical grade) under adjustment by a pH meter. Quantum yield (Φ) were calculated according to the literature procedure.[23]

Density functional optimizations were carried out using Gamess.[24] The geometries of each of the compounds were optimized using density functional theory (DFT) with B3-LYP functional[25] at the 6-31G (d,p) basis set. The excited state electronic transition calculations were done using time-dependent density functional theory (TD-DFT)[26] with the same functional and basis set using a suite of Gaussian 03 programs.

4.2. Calculation of binding constant

The binding constant (K_a) value of **3** and **4** with Cu^{2+} was determined from the emission intensity data following the steady-state fluorometric method[15] in which I_0 refer to the intensities of fluorescence of the solutions containing free ligand. From the fluorescence titration when $I_0/(I-I_0)$ is plotted against the reciprocal of the cation concentration ($1/[M]$) the stability constant is obtained from the ratio intercept/slope with a good linear correlation coefficient (R=0.98647 for **3** and 0.99027 for **4**) as shown in Fig. 7.

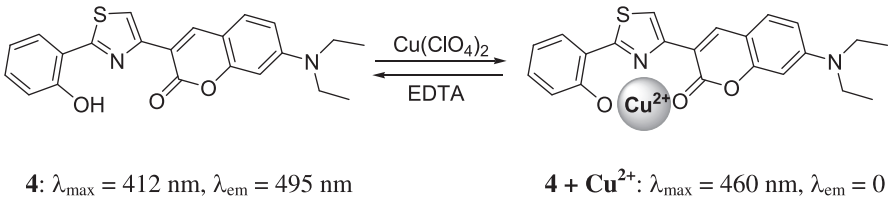

4: λ_{max} = 412 nm, λ_{em} = 495 nm

4 + Cu^{2+}: λ_{max} = 460 nm, λ_{em} = 0

Scheme 2.

3. Conclusion

In summary, we have developed a new thiazole-coumarin based highly selective, sensitive, reversible, chromogenic, and fluorogenic chemosensor **4** for copper ions in aqueous-DMSO (3:1) containing HEPES buffer (10 mM, pH 7.4). It utilizes strong coordination of copper cations on the phenolic oxygen, thiazole nitrogen, and carbonyl oxygen atom in coumarin. Introduction of an electron-donating diethylamino group to the coumarin ring enhanced the ICT. Chemosensor **4** also exhibits fluorescence quenching upon binding of Cu^{2+} ion with an "on–off' type fluoroionophoric switching property. Its fluorescent signal can be revived by the addition of an EDTA solution. Finally, we have also elaborated on the mechanism of fluorescence quenching in terms of the occupancy of the frontier orbitals.

4. Experimental section

4.1. General methods

Melting points were determined using a Thomas-Hoover capillary melting point apparatus and are uncorrected. The ^1H and ^{13}C NMR spectra were recorded on a Bruker AM-400 spectrometer using Me_4Si as the internal standard. FAB mass and EPR were taken at KBSI Daegu branch. The UV–vis absorption spectra were determined on a Shimadzu UV-1650PC spectrophotometer. Fluorescence spectra were measured on a Shimadzu RF-5301 fluorescence spectrometer equipped with a xenon discharge lamp and 1 cm quartz cells. All of the measurements were operated at 298 K.

4.3. Calculation of detection limit

The fluorescence spectra of the chemosensor **4** in various concentrations of free Cu^{2+} were normalized between the maximum and the minimum intensities as shown in Fig S6. A linear regression curve was fitted to the eight intermediate values. The point at which this line crossed the ordinate axis was taken as the detection limit and equaled approximately 0.04 μM of Cu^{2+}.[22]

4.4. Synthesis of chemosensor

*4.4.1. Chemosensor **3**.* A solution of 2-hydroxythiobenzamide (**6**, 200 mg, 1.48 mmol) and 3-(2′-bromoacetyl)coumarin (**7**, 470 mg, 1.78 mmol) in ethanol (15 mL) was refluxed for 2 h. The reaction progress was monitored by TLC analysis. The solvent was removed in vacuo and the residue was washed with water, neutralized with 1 N NaOH and extracted with EtOAc. The organic layer was dried over anhydrous Na_2SO_4 and concentrated. The residue was purified by column chromatography (10% EtOAc in hexane) to give **3** in 90% yield. Mp 142–143 °C. ^1H NMR (DMSO-d_6) δ 6.98 (t, J=7.6 Hz, 1H), 7.04 (d, J=8.4 Hz, 1H), 7.42–7.30 (m, 3H), 7.59 (t, J=8.4 Hz, 1H), 7.90 (d, J=8.0 Hz, 1H), 8.32 (dd, J=8.0, 1.5 Hz, 1H), 8.40 (s, 1H), 8.90

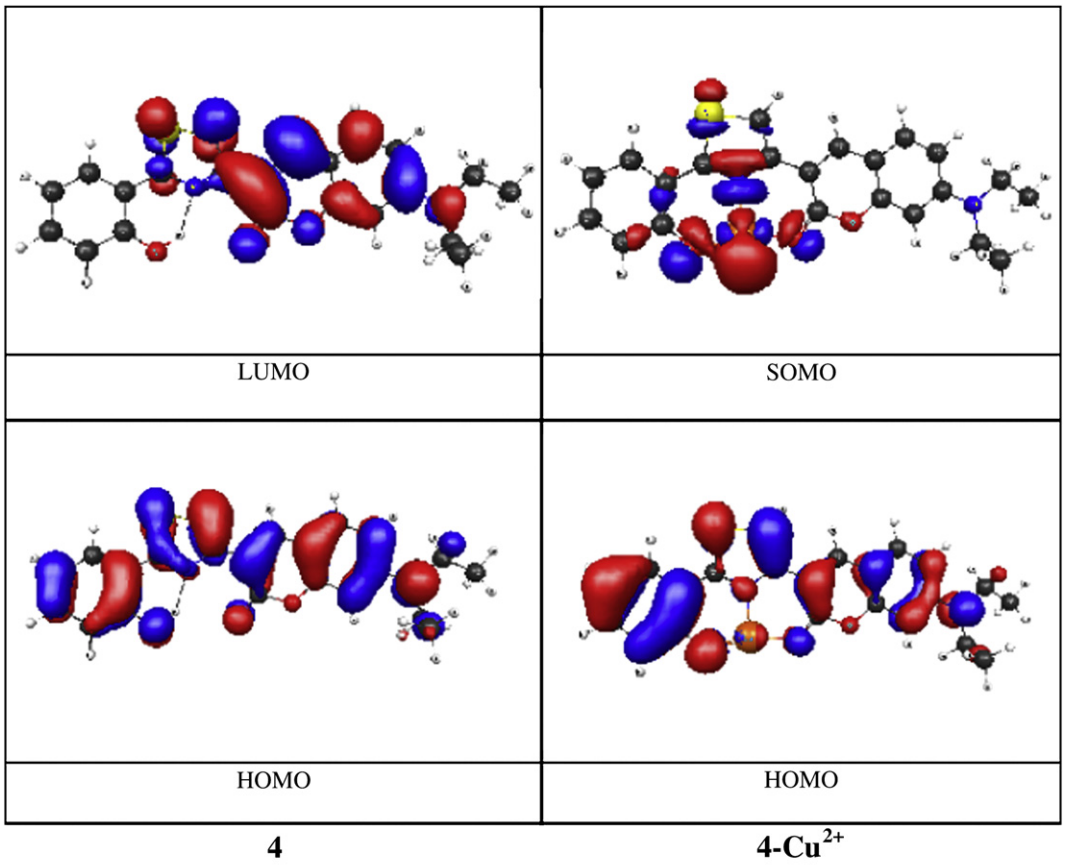

Fig. 11. B3LYP/6-31G* calculated molecular orbitals of **4** and **4**–Cu^{2+}.

Table 2
The contributions of each electronic oscillator (orbital transitions) to the lowest energy transition

Electronic oscillators	**4** (%)	Electronic oscillators	**4**–Cu^{2+} (%)
H-1→L	22.70	H-16→S	7.41
H→L	62.41	H-8→S	19.75
H-1→L+1	4.96	H-1→S	19.14
H→L+1	9.93	H→S	53.70

Table 3
The TD-B3LYP/6-31G(d) calculated oscillator strength f_1 to the lowest energy transition

	3	**3**–Cu^{2+}	**4**	**4**–Cu^{2+}
f_1	0.050	0.0004	0.345	0.0001

(s, 1H), 11.17 (s, 1H, OH); ^{13}C NMR (DMSO-d_6) δ 115.8, 116.5, 118.9, 119.2, 119.4, 120.1, 120.2, 124.7, 127.8, 128.9, 131.2, 131.8, 139.3, 146.1, 152.5, 155.2, 158.9, 162.6. Anal. Calcd for $C_{18}H_{11}NO_3S$: C, 67.28; H, 3.45; N, 4.36; S, 9.98. Found C, 67.24; H, 3.33; N, 4.35; S, 9.58.

4.4.2. Chemosensor ***4***. This compound was obtained by the same procedure as above using 2-hydroxythiobenzamide (**6**, 200 mg, 1.3 mmol) and 3-(2′-bromoacetyl)-7-diethylaminocoumarin (**8**, 530 mg, 1.6 mmol) in ethanol (15 mL). The product was purified by column chromatography (25% EtOAc in hexane) to give **4** in 68% yield. Mp 164–165 °C. ^{1}H NMR (DMSO-d_6) δ 1.12 (t, J=7.0 Hz, 6H), 3.43 (q, J=7.1 Hz, 4H), 6.56 (d, J=2.0 Hz, 1H), 6.73 (dd, J=8.8, 2.2 Hz, 1H), 6.99 (t, J=7.8 Hz, 1H), 7.05 (d, J=7.8 Hz, 1H), 7.33 (dt, J=8.3, 1.8 Hz, 1H), 7.64 (d, J=9.1 Hz, 1H), 8.23 (s, 1H), 8.29 (dd, J=7.8, 1.7 Hz, 1H), 8.75 (s, 1H), 11.22 (s, 1H, OH); ^{13}C NMR (DMSO-d_6) δ 12.4, 44.1, 96.0, 108.0, 109.4, 112.8, 116.6, 116.9, 119.0, 119.5, 127.7, 130.1, 131.1, 140.2, 147.4, 150.7, 155.2, 155.6, 159.9, 162.4. Anal. Calcd for $C_{22}H_{20}N_2O_3S$: C, 67.33; H, 5.14; N, 7.14; S, 8.17. Found C, 67.04; H, 5.19; N, 7.15; S, 7.90.

4.4.3. Chemosensor ***5***. This compound was obtained by the same procedure as above using thiobenzamide (**9**, 200 mg, 1.4 mmol) and **8** (530 mg, 1.6 mmol) in ethanol (15 mL). The product was purified by column chromatography (10% EtOAc in hexane) to give **5** in 68% yield. Mp 155–156 °C. ^{1}H NMR ($CDCl_3$) δ 1.22 (t, J=7.0 Hz, 6H), 3.41 (q, J=7.1 Hz, 4H), 6.53 (s, 1H), 6.63 (d, J=8.0 Hz, 1H), 7.42 (d, J=8.8 Hz, 1H), 7.45 (t, J=7.3 Hz, 3H), 8.04 (d, J=8.0 Hz, 2H), 8.29 (s, 1H), 8.73 (s, 1H); ^{13}C NMR ($CDCl_3$) δ 12.5, 44.9, 97.1, 109.0, 109.4, 114.4, 116.8, 126.6, 128.9, 129.6, 130.0, 133.7, 140.6, 149.9, 150.6, 155.9, 160.9, 166.7. Anal. Calcd for $C_{22}H_{20}N_2O_2S$: C, 70.19; H, 5.35; N, 7.44; S, 8.52. Found C, 69.70; H, 5.53; N, 7.39; S, 8.31.

*4.4.4. Cu^{2+}–**4** complex.* A mixture of **4** (100 mg, 0.25 mmol) and Cu $(ClO_4)_2\cdot 6H_2O$ (110 mg, 0.29 mmol) in ethanol–DMSO (v/v 9:1, 5 mL) was refluxed for 6 h. The mixture was cooled to room temperature and the precipitated complex was filtered. The filtered cake was washed thoroughly with water, ethanol, and dried under vacuum to provide the complex (100 mg, 74% yield). HR-FAB mass: calcd for ($C_{22}H_{19}O_3N_2S\cdot Cu\cdot DMSO$) 532.0552; found: 532.0557.

Acknowledgements

This research was supported by the Basic Science Research Program through the National Research Foundation of Korea (NRF), and funded by the Ministry of Education, Science, and Technology (20100010070). The Research Institute of Industrial Technology at Kyungpook National University also supported A.H.

Supplementary data

Supplementary data associated with this article can be found in online version at doi:10.1016/j.tet.2011.01.093. These data include MOL files and InChiKeys of the most important compounds described in this article.

References and notes

1. (a) de Silva, A. P.; Gunaratne, H. Q. N.; Gunnlaugsson, T.; Huxley, A. J. M.; McCoy, C. P.; Rademacher, J. T.; Rice, T. E *Chem. Rev.* **1997**, *97*, 1515; (b) Valeur, B.; Leray, I *Coord. Chem. Rev.* **2000**, *205*, 3; (c) de Silva, A. P.; Fox, D. B.; Huxley, A. J. M.; Moody, T. S *Coord. Chem. Rev.* **2000**, *205*, 41; (d) Prodi, L.; Bolletta, F.; Montalti, M.; Zaccheroni, N *Coord. Chem. Rev.* **2000**, *205*, 59.
2. (a) Gunnlaugsson, T.; Leonard, J. P.; Murray, N. S *Org. Lett.* **2004**, *6*, 1557; (b) Xu, Z. C.; Qian, X. H.; Cui, J. N *Org. Lett.* **2005**, *7*, 3029; (c) Xiang, Y.; Tong, A. J *Org. Lett.* **2006**, *8*, 1549; (d) Xiang, Y.; Tong, A. J.; Jin, P. Y.; Ju, Y *Org. Lett.* **2006**, *8*, 2863; (e) Martinez, R.; Zapata, F.; Caballero, A.; Molina, P *Org. Lett.* **2006**, *8*, 3235; (f) Wang, J. B.; Qian, X. H.; Cui, J. N *J. Org. Chem.* **2006**, *71*, 4308; (g) Gunnlaugsson, T.; Leonard, J. P *J. Chem. Soc., Perkin Trans. 2* **2002**, 1980.
3. Tak, W. T.; Yoon, S. C *KSN* **2001**, *20*, 863.
4. (a) Barceloux, D. G *J. Toxicol., Clin. Toxicol.* **1999**, *37*, 217; (b) Mathie, A.; Sutton, G. L.; Clarke, C. E.; Veale, E. L *Pharmacol. Ther.* **2006**, *111*, 567; (c) Kim, B.-E.; Nevitt, T.; Thiele, D. J *Nat. Chem. Biol.* **2008**, *4*, 176.
5. (a) Mare, S.; Penugonda, S.; Robinson, S. M.; Dohgu, S.; Banks, W. A.; Ercal, N *Peptides* **2007**, *28*, 1424; (b) Deraeve, C.; Boldron, C.; Maraval, A.; Mazarguil, H.; Gornitzka, H.; Vendier, L.; Pitié, M.; Meunier, B *Chem.—Eur. J.* **2008**, *14*, 682; (c) Lee, J. C.; Gray, H. B.; Winkler, J. R *J. Am. Chem. Soc.* **2008**, *130*, 6898.
6. (a) He, G.; Zhang, X.; He, C.; Zhao, X.; Duan, C *Tetrahedron* **2010**, *66*, 9762; (b) Du, J.; Fan, J.; Peng, X.; Sun, P.; Wang, J.; Li, H.; Sun, S *Org. Lett.* **2010**, *12*, 476; (c) Yu, C.; Zhang, J.; Wang, R.; Chen, L *Org. Biomol. Chem.* **2010**, *8*, 5277; (d) Jung, H. S.; Kwon, P. S.; Lee, J. W.; Kim, J., II; Hong, C. S.; Kim, J. W.; Yan, S.; Lee, J. Y.; Lee, J. H.; Joo, T.; Kim, J. S *J. Am. Chem. Soc.* **2009**, *131*, 2008; (e) Kim, H. J.; Hong, J.; Hong, A.; Ham, S.; Lee, J. H.; Kim, J. S *Org. Lett.* **2008**, *10*, 1963; (f) Dhir, A.; Bhalla, V.; Kumar, M *Tetrahedron Lett.* **2008**, *49*, 4227; (g) Kim, H. J.; Park, S. Y.; Yoon, S.; Kim, J. S *Tetrahedron* **2008**, *64*, 1294; (h) Sheng, R.; Wang, P.; Gao, Y.; Wu, Y.; Liu, W.; Ma, J.; Li, H.; Wu, S *Org. Lett.* **2008**, *10*, 5015; (i) Kumar, S.; Kaur, N *Supramol. Chem.* **2006**, *18*, 137; (j) Kim, H. J.; Bok, J. H.; Vicens, J.; Suh, I.-H.; Ko, J.; Kim, J. S *Tetrahedron Lett.* **2005**, *46*, 8765; (k) Zheng, Y.; Cao, X.; Orbulescu, J.; Konka, V.; Andreopoulos, F. M.; Pham, S. M.; Leblanc, R. M *Anal. Chem.* **2003**, *75*, 1706.
7. Wang, H.-H.; Xue, L.; Fang, Z.-J.; Li, G.-P.; Jiang, H *New J. Chem.* **2010**, *34*, 1239 and the references there in.
8. (a) Leray, I.; Asfari, Z.; Vicens, J.; Valeur, B *J. Chem. Soc., Perkin Trans. 2* **2002**, 1429; (b) Chen, C.-T.; Huang, W.-P *J. Am. Chem. Soc.* **2002**, *124*, 6246; (c) Ray, D.; Bharadwaj, P. K *Inorg. Chem.* **2008**, *47*, 2252; (d) Lee, M. H.; Quang, D. T.; Jung, H. S.; Yoon, J.; Lee, C.-H.; Kim, J. S *J. Org. Chem.* **2007**, *72*, 4242.
9. Yoon, S.; Albers, A. E.; Wong, A. P.; Chang, C. J. *J. Am. Chem. Soc.* **2005**, *127*, 16030.
10. Moylan, C. R *J. Phys. Chem.* **1994**, *98*, 13513.
11. (a) Krämer, R *Angew. Chem., Int. Ed.* **1998**, *37*, 772; (b) Chen, X.; Li, Z.; Xiang, Y.; Tong, A *Tetrahedron Lett.* **2008**, *49*, 4697.
12. Helal, A.; Kim, H.-S *Tetrahedron Lett.* **2009**, *50*, 5510.
13. Helal, A.; Lee, S. H.; Kim, S. H.; Kim, H.-S. *Tetrahedron Lett.* **2010**, *51*, 3531.
14. Takechi, H.; Oda, Y.; Nishizono, N.; Oda, K.; Machida, M *Chem. Pharm. Bull.* **2000**, *48*, 1702.
15. (a) Connors, K. A *Binding Constants: The Measurement of Molecular Complex Stability*; Wiley: New York, NY, 1987, pp 21–101, 339–343; (b) Forgues, S. F.; LeBris, M. T.; Gutte, J. P.; Valuer, B *J. Phys. Chem.* **1988**, *92*, 6233; (c) Thordarson, P. *Chem. Soc. Rev.* **2011**, *40*, 1305.
16. (a) Atkins, R. L.; Bliss, D. E *J. Org. Chem.* **1978**, *43*, 1975; (b) Fletcher, A. N.; Bliss, D. E *Appl. Phys.* **1978**, *16*, 289; (c) Halstead, J. A.; Reeves, R. R *Opt. Commun.* **1978**, *27*, 273; (d) Fletcher, A. N *Appl. Phys.* **1977**, *14*, 295.
17. Klymchenko, A. S.; Ozturk, T.; Pivovarenko, V. G.; Demchenko, A. P *Tetrahedron Lett.* **2001**, *42*, 7967.
18. (a) Kobayashi, H.; Ogawa, M.; Alford, R.; Choyke, P. L.; Urano, Y *Chem. Rev.* **2010**, *110*, 2620; (b) Dujols, V.; Ford, F.; Czarnik, A. W *J. Am. Chem. Soc.* **1997**, *119*, 7386; (c) Gunnlaugsson, T.; Leonard, J. P.; Senechal, K.; Harte, A. J *Chem. Commun.* **2004**, 782; (d) Klein, G.; Kaufmann, D.; Schurch, S; Reymond, J-L. *Chem. Commun.* **2001**, 561.
19. (a) Wu, Q.; Anslyn, E. V. *J. Am. Chem. Soc.* **2004**, *126*, 14682; (b) Zeng, H. H.; Thompson, R. B.; Maliwal, B. P.; Fones, G. R.; Moffett, J. W.; Fierke, C. A *Anal. Chem.* **2003**, *75*, 6807; (c) Rurack, K. *Spectrochim. Acta, Part A* **2001**, *57*, 2161; (d) Kavallieratos, K.; Rosenberg, J. M.; Chen, W.-Z.; Ren, T *J. Am. Chem. Soc.* **2005**, *127*, 6514; (e) Zheng, Y.; Orbulescu, J.; Ji, X.; Andreopoulos, F. M.; Pham, S. M.; Leblanc, R. M *J. Am. Chem. Soc.* **2003**, *125*, 2680; (f) Quang, D. T.; Jung, H. S.; Yoon, J. H.; Lee, S. Y.; Kim, J. S *Bull. Korean Chem. Soc.* **2007**, *28*, 682.
20. Fabbrizzi, L.; Licchelli, M.; Pallavicini, P.; Parodi, L.; Taglietti, A Transition metals in supramolecular chemistry In *Fluorescent Sensors for and with Transition Metals*; Sauvage, J. P., Ed.; John Wiley: Chichester, UK, 1999.
21. Ci, Y. X.; Zhou, T. Z *The Coordinated Complexes in Analytical Chemistry*; Peking University: Beijing, 1984.
22. Shortreed, M.; Kopelman, R.; Kuhn, M.; Hoyland, B *Anal. Chem.* **1996**, *68*, 1414.
23. Helal, A.; Kim, S. H.; Kim, H.-S *Tetrahedron* **2010**, *66*, 9925.
24. (a) Schmidt, M. W.; Balbridge, K. K.; Boatz, J. A.; Elbert, S. T.; Gordon, M. S.; Jensen, J. H.; Koseki, S.; Matsunaga, N.; Nguyen, K. A.; Su, S.; Windus, T. L.; Dupuis, M.; Montgomery, J. A., Jr. *J. Comput. Chem.* **1993**, *14*, 1347; (b) Fletcher, G. D.; Schmidt, M. W.; Gordon, M. S. *Adv. Chem. Phys.* **1999**, *110*, 267.
25. Becke, A. D. *J. Chem. Phys.* **1993**, *98*, 5648.
26. Dreuw, A.; Head-Gordon, M. *Chem. Rev.* **2005**, *105*, 4009.